

Supporting information
for
Single Ultrabright Fluorescent Silica Nanoparticles Can Be Used as
Individual Fast Real-Time Nanothermometers

Mahshid Iraniparast,¹, Nishant Kumar,¹ Igor Sokolov^{1,2,3,*}

¹ *Department of Mechanical Engineering, Tufts University, Medford, MA 02155, USA;*

² *Department of Biomedical Engineering, Tufts University, Medford, MA 02155, USA.*

³ *Department of Physics, Tufts University, Tufts University, Medford, MA 02155, USA.*

Calculating the number of dye molecules within each nanoparticle

The Beer–Lambert law was employed to calculate the number of dye molecules per volume in this study. The UV-Vis absorbance of nanoparticles encapsulated with R6G and RB was measured for this purpose. The extinction coefficients of R6G and RB, as referenced in the previous study (ref. 33 the manuscript), were used in determining the concentration of each of the dye molecules. The result showed 3.91×10^{13} of R6G and 4.71×10^{13} of RB per volume.

Subsequently, the total number of particles per volume was calculated based on the density, weight, and volume of nanoparticles. The resulting total number of particles was determined to be 3.087×10^{10} per volume. Dividing the total number of dye molecules per volume by the total number of particles per volume yielded the number of dye molecules per particle. The detailed results are presented in the main content of the study. The whole calculation is described below:

$$\text{Beer Law: } A = \varepsilon \times C \times L$$

$$0.005865 = 90300 \times C \times 1$$

$$C = 6.49 \times 10^{-8} \text{ (Mol)}$$

$$\begin{aligned} \text{Number of R6G dye molecules per volume: } & 6.49 \times 10^{-8} \times 6.022 \times 10^{23} \times 10^{-3} \\ & = 3.91 \times 10^{13} \end{aligned}$$

$$\begin{aligned} \text{Weight of one particle: } & \rho \times \frac{4}{3} \times \pi \times R^3 = 1600 \times \frac{4}{3} \times \pi \times \left(\frac{43}{2}\right)^3 \times 10^{-6} \\ & = 6.663 \times 10^{-14} \text{ (mg)} \end{aligned}$$

$$\text{Number of particles per volume: } \frac{\frac{(12 \times 0.001 \times 0.6)}{3.5}}{6.663 \times 10^{-14}} = 30872067297$$

$$\text{Number of R6G per each nanoparticle: } \frac{3.9119 \times 10^{13}}{30872067297} = 1267.1482$$

The same approach was used for calculation of number of RB molecules within each nanoparticle:

$$\text{Beer Law: } A = \varepsilon \times C \times L$$

$$0.00735 = 94000 \times C \times 1$$

$$C = 7.819 \times 10^{-8} \text{ (Mol)}$$

$$\begin{aligned} \text{Number of RB dye molecules per volume: } & 7.819 \times 10^{-8} \times 6.022 \times 10^{23} \times 10^{-3} \\ & = 4.7094 \times 10^{13} \end{aligned}$$

$$\begin{aligned} \text{Weight of one particle: } & \rho \times \frac{4}{3} \times \pi \times R^3 = 1600 \times \frac{4}{3} \times \pi \times \left(\frac{43}{2}\right)^3 \times 10^{-6} \\ & = 6.663 \times 10^{-14} \text{ (mg)} \end{aligned}$$

$$\text{Number of particles per volume: } \frac{\frac{(12 \times 0.001 \times 0.6)}{3.5}}{6.663 \times 10^{-14}} = 30872067297$$

$$\text{Number of RB per each nanoparticle: } \frac{4.7094 \times 10^{13}}{30872067297} = 1525.4804$$

Calculating the fluorescence brightness of the nanothermometers

The brightness of individual nanoparticles was determined by calculating their relative brightness compared to standard fluorophores. In this case, the standard fluorophores are naturally free rhodamine 6G and B dyes dissolved in water. It well describes the brightness of the particles at different wavelengths because the fluorescent spectra of individual dye molecules are almost unchanged after encapsulation. Specifically, the fluorescence spectra of rhodamine 6G after encapsulation have a small redshift of about 5 nm, whereas rhodamine B demonstrates a blueshift of 3 nm.^{1,2} The used unit of measurement for brightness is MESF (Molecules of Equivalent Soluble Fluorochrome), and it is obtained using the following equation:

$$\text{Relative Brightness} = \frac{FL_{NPs} / \text{Number of nanoparticles}}{FL_{dye} / \text{Number of dye molecules}}$$

Here, FL_{NPs} and FL_{dye} represents the fluorescence intensity of nanoparticles and dye molecules, respectively. The brightness was calculated separately for each of the two molecules, R6G and RB, and the results are mentioned in the main content.

Measurements of laser power density used for the imaging in scanning laser confocal microscope

The laser power produced by the supercontinuum laser of the Leica laser scanning confocal microscope was measured using a Thorlabs power meter tuned for the excitation wavelengths of 488 nm. The detection head was placed right above the microscope (inverse) 40x, 1.3 NA objective. The distance between the head and the objective was chosen to maximize the power reading (and it was constant with at least ~2mm interval of the distances). The power was measured at several positions of the laser power control: 2, 3, 4, 8% (the percentage of the total working power of the microscope laser). All measurements presented in the paper were down at the 2% of the laser power (with the exception of the measurements of the dependence of the fluorescence ratio on the laser power). The results are presented in Table S1.

Table S1. The results of the measurements of the laser power and laser power density of the super continuum laser used in the Leica laser scanning confocal microscope.

Laser power control %	Measured power [μW]	Power density W/cm^2
2	0.7	425
3	1.1	638
4	1.4	850
8	2.8	1700

The power density was calculated as the measured power divided by the size of the laser spot, which is the airy disc = $1.22 \lambda/\text{NA}$, where $\lambda=488 \text{ nm}$, $\text{NA}=1.3$. Note that the same method was used in the paper which reported the previous record [reference 18 of the main text].

Calculation of the temperature resolution

An example of fitting of temperature fluctuations σ_T versus the time of measurement t_m is shown in figure S1a. The measured temperature resolutions from individual nanoparticles are presented in Figure S1b. It is important to stress that this quite noticeable spread of the temperature resolutions (Figure S1b) does not have a direct relation to the accuracy of the conversion of the fluorescence ratio to temperature, which can be presented by the relative sensitivity. This is because the spread of temperature resolutions is defined by the total number of fluorescent molecules in each particle, or the volume of the particle. For example, a large particle could be considered as several smaller particles together. As one can see from Figure 3c, the larger number of particles, the smaller the temperature uncertainty (simply due to the ergodic averaging), and consequently, the higher temperature resolution (see, also Fig.4a). If the dye molecules are spread evenly through the particle volume, the accuracy of finding temperature using the described ratiometric approach is independent of the particle volume. Indirectly, it manifests itself by the narrowness of the relative sensitivity, Figure 3b.

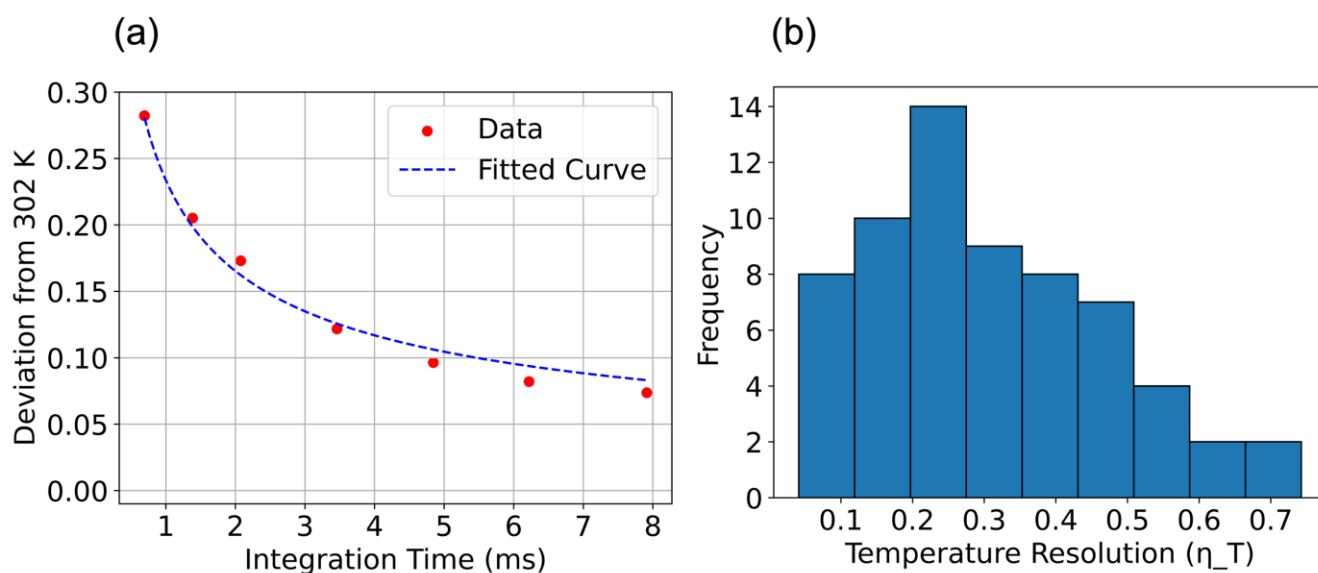


Figure S1. Calculation of the temperature resolution η_T . (a) an example of fitting of temperature fluctuations σ_T versus the time of measurement t_m . (b) The histogram of the temperature resolutions for individual nanothermometers. Sixty individual nanoparticles were investigated. The mode and average are $0.25 \text{ K.Hz}^{-1/2}$ and $0.30 \text{ K.Hz}^{-1/2}$, respectively. All the measurements were performed using excitation power density of $455 \text{ (w. cm}^{-2}\text{)}$.

Calculation of fluorescence ratio – temperature dependence

The measured data is shown in figure S2. The temperature dependence was calculated using the mean least square method using the measurement data shown in Figure S2. Formula

$Temperature = 10.3 \times Ratio + 293$ was derived for the linear regression of the mean least square method.

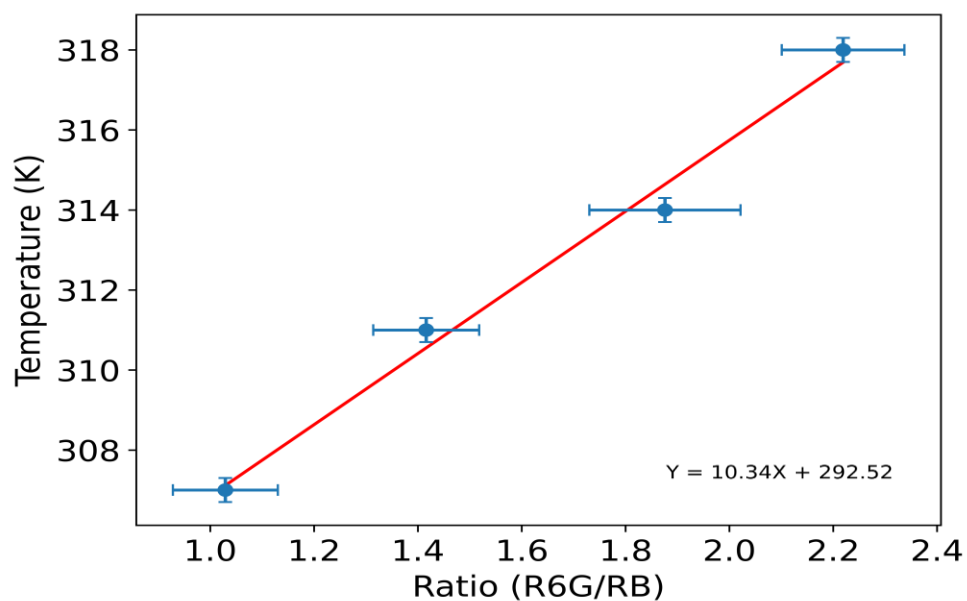


Figure S2. The fluorescence ratio for the individual nanothermometers upon changing temperature. The plot demonstrates a linear relationship between the change in the R6G to RB fluorescence intensity ratio and temperature. Each data point is calculated for ten different nanothermometers; the fluorescence signal was collected for 20 ms for each nanothermometer. This data was collected using the laser scanning confocal microscope (Leica).

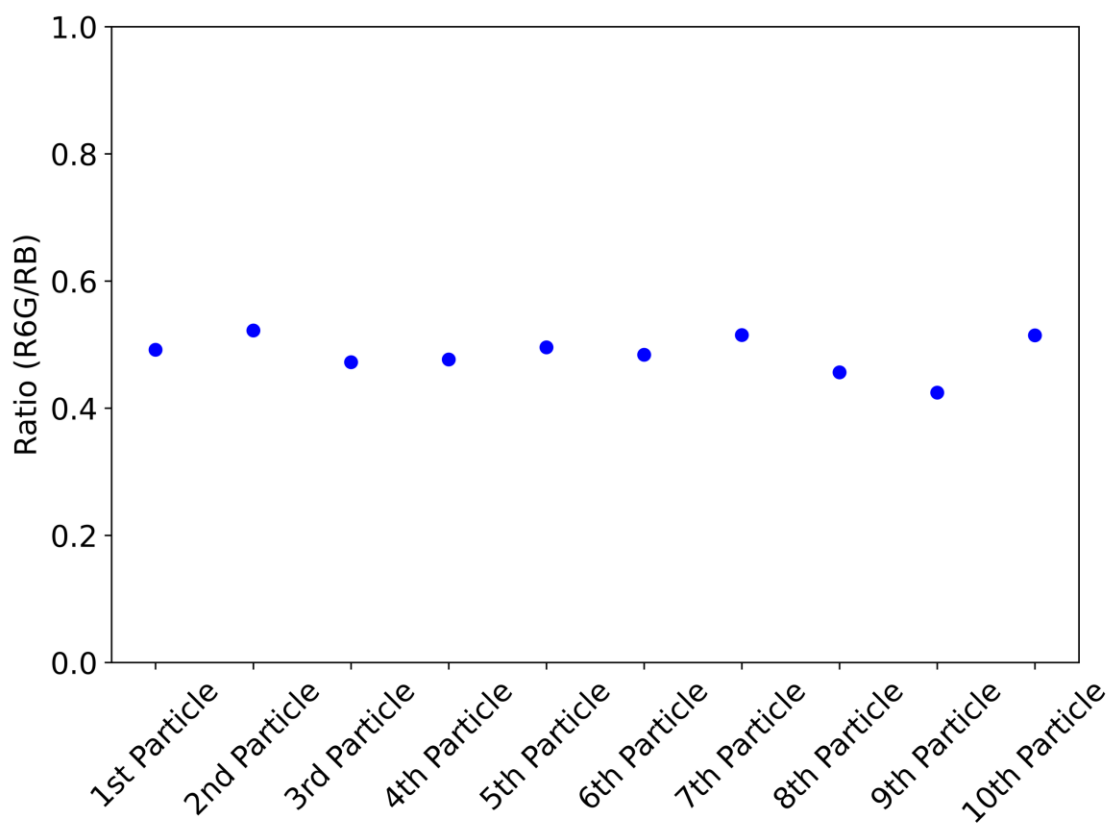


Figure S3: Fluorescence intensity of R6G to RB ratio of 10 random individual nanothermometers. This graph is prepared using the data shown in figure 3b. The collection time for each nano thermometer was 30 ms. These data were collected using the Raman confocal microscope.

Photoluminescence stability of the nanothermometers

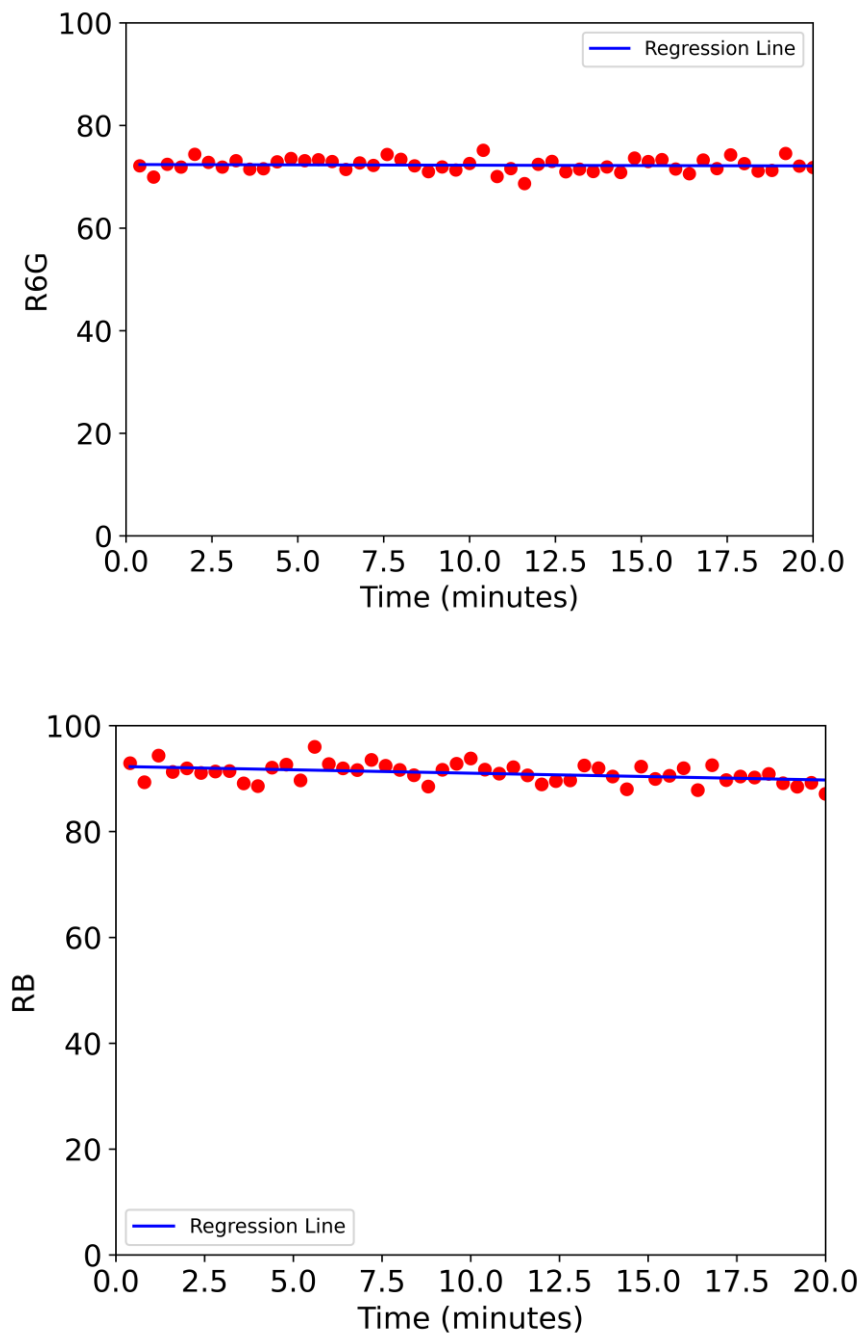


Figure S4: Photoluminescence stability: Fluorescence intensity of the measured nanothermometers integrated in the spectral range of R6G dye (510 nm - 560 nm) and RB dye (560 nm - 580 nm).

Demonstration of the presence of the Förster resonance energy transfer (FRET) between the dyes encapsulated inside of the nanothermometers

R6G and RB dyes were dissolved in water in the same proportion as encapsulated inside the nanothermometers. The emission–correlation matrices are shown in supplementary Figure S5 for both water-diluted dyes and the same proportion of the dyes encapsulated in the nanothermometers. To ensure that there was no FRET in the water-dissolved dyes, the concentration of the dyes was $\sim 10^3$ lower compared to the dyes encapsulated in the particles (of the order of micromoles). One can see from supplementary figure S5 that the fluorescence emitted by R6G molecules is substantially depleted in the case of the dyes encapsulated inside nanoparticles, whereas the fluorescence intensity of RB dye is substantially increased. This is what should be expected as a result of FRET: R6G serves as a donor, which transfers its energy to the acceptor, RB dye.

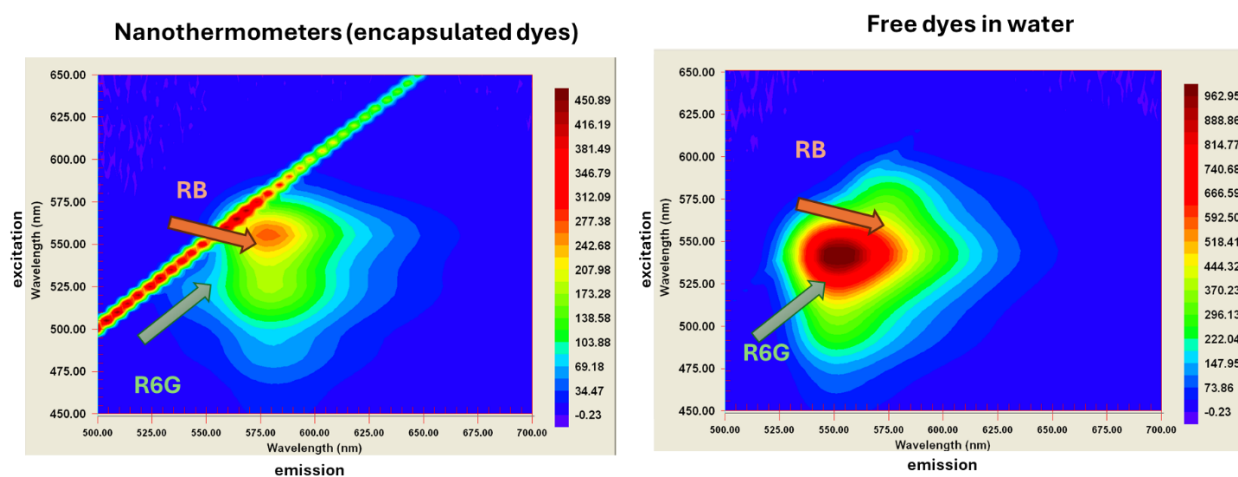


Figure S5: The emission-excitation matrix of the mix of the two dyes encapsulated inside the nanothermometers and dissolved in water. Dyes were dissolved in water at the same proportion as encapsulated inside the nanothermometers. The arrow shows the directions towards the location of RB and R6G peaks. (The absence of clear locations of individual peaks are explained by the spectral overlap between the two dyes.)

Another reason for FRET can be given by estimating the distances between the dye molecules inside of each particle. To calculate it, we assume a homogeneous distribution of the dye molecules across the silica matrix of the nanoparticle (which is a reasonable assumption; see

ref. 31 the manuscript). Taking the average diameter of the particle of 43 nm and the total number of molecules per particle to be 2800 (1270 of R6G and 1530 of RB molecules), one can obtain the average distance between the molecules of 5 nm. On the other hand, one can estimate the distance between molecules assuming that they are located in the cylindrical silica channels inside the particle. It is characterized by the DFT pore diameter of 3.8 nm, and the available pore volume of 0.75 cm³/g (ref. 35 the manuscript). Assuming a homogeneous distribution of the same number of dye molecules along the cylindrical channels, one can obtain an average distance between the dye molecules of 1.6 nm. If we assume for simplicity that each pair of these molecules is donor and acceptor, we can obtain the FRET efficiency using the equation:

$$\text{Efficiency} = R_0^6 / (R_0^6 + r^6), \quad (\text{S1})$$

where R_0 is the Förster distance and r is the distance between dye molecules. R_0 was calculated to be 8.79 nm (see, e.g., ref. 32 of the manuscript), considering the emission spectrum of R6G dye as a donor and the absorbance spectrum of RB as an acceptor. Using this equation, one can estimate the FRET efficiency as 97-100%.

However, the above estimation is not entirely correct. It can only be referred to as the ideal case of close proximity of donor and acceptor molecules. When speaking about FRET efficiency between molecules encapsulated in a nanoparticle, one has to take into account the random location of the molecules, which results in a limited number of donor – acceptor pairs. As was shown as a result of statistical simulations in ¹ (ref. 33 the manuscript), the effective FRET between R6G and RB dyes encapsulated inside of a nanoparticle is substantially smaller than the estimated using the idealized case of donor-acceptor pairs. Running the simulations described in ¹ for the number of dye molecules measured in this work, one can find the efficiency FRET has ~41% efficiency.

Finally, FRET can also be estimated using the following formula:

$$\text{Efficiency} = 100\% * \left(1 - \frac{FI_{in\ presence\ of\ acceptor}}{FI_{no\ acceptor}}\right), \quad (\text{S2})$$

where $FI_{in\ presence\ of\ acceptor}$ is the fluorescence intensity in the presence of the acceptor, and $FI_{no\ acceptor}$ is that in the absence of the acceptor. The mesoporous silica nanoparticles particles containing only donor (R6G) in the appropriate concentrations range were investigated in ² (ref. 31 of the manuscript). Although such high concentrations were not reached in ², one can see a

linear dependence between the dye concentration and brightness of mesoporous silica nanoparticles containing R6G (Fig.2 of ref. ²), we can estimate the brightness of such particles containing 1270 molecules of R6G as 1050 (Brightness relative to one molecule of R6G). Therefore, one can estimate $FI_{no\ acceptor} = 1050$. The brightness of the particles reported here (which contain 1270 molecules of R6G in presence of RB acceptor) is equal to 650 in the same units. It gives the efficiency of FRET of 36%, which is in relatively good agreement with the results of the simulations given above.

References

1. M. Iraniparast, B. R. Peng and I. Sokolov, *Sensors-Basel*, 2023, **23**.
2. V. Kalaparthi, S. Palantavida and I. Sokolov, *J. Mater. Chem. C*, 2016, **4**, 2197-2210.